RAA 2020 Vol. **20** No. **9**, 150(10pp) doi: 10.1088/1674–4527/20/9/150
© 2020 National Astronomical Observatories, CAS and IOP Publishing Ltd.
http://www.raa-journal.org *http://iopscience.iop.org/raa*

***R**esearch in*
***A**stronomy and*
***A**strophysics*

The evolutionary status of chemically peculiar eclipsing binary star DV Boo

Filiz Kahraman Aliçavuş[1,2] and F. Aliçavuş[1]

[1] Çanakkale Onsekiz Mart University, Faculty of Sciences and Arts, Physics Department, 17100, Çanakkale, Turkey; *filizkahraman01@gmail.com*
[2] Nicolaus Copernicus Astronomical Center, Bartycka 18, PL-00-716 Warsaw, Poland

Received 2019 December 16; accepted 2020 April 26

Abstract Eclipsing binary systems are unique stellar objects to examine and understand stellar evolution and formation. Thanks to these systems, the fundamental stellar parameters (mass, radius) can be obtained very precisely. The existence of metallic-line (Am) stars in binaries is noticeably common. However, the known number of Am stars in eclipsing binaries is less. The Am stars in eclipsing binaries are extremely useful to deeply investigate the properties of Am stars, as eclipsing binaries are the only tool to directly derive the fundamental stellar parameters. Additionally, the atmospheric parameters and metallicities of such binary components could be obtained by a detailed spectroscopic study. Therefore, in this study, we present a comprehensive photometric and spectroscopic analysis of the eclipsing binary system DV Boo which has a possible Am component. The fundamental stellar parameters were determined by the analysis of radial velocity and photometric light curves. The atmospheric parameters of both binary components of DV Boo were derived considering the disentangled spectra. The chemical abundance analysis was carried out as well. As a result, we showed that the primary component exhibits a typical Am star chemical abundance distribution. The fundamental stellar parameters of the binary components were also obtained with an accuracy of $<$1% for masses and $<$3% for radii. The evolutionary status of DV Boo was examined utilizing the precisely obtained stellar parameters. The age of the system was found to be 1.00 ± 0.08 Gyr.

Key words: techniques: photometric : spectroscopic — stars: variables: binaries: eclipsing: fundamental parameters — stars: individual: DV Boo

1 INTRODUCTION

A significant amount of stars are members of binary or multiple systems (Alfonso-Garzón et al. 2014; Sana & Evans 2011). These objects, in particular the eclipsing binary systems, are unique tools to acquire information about the formation and evolution of stars. Eclipsing binary systems provide a direct measurement of the fundamental stellar parameters (e.g., mass, radii) with a good accuracy (Torres et al. 2010; Southworth 2013). These fundamental parameters are significant for a deep investigation of a star. To obtain the precise fundamental stellar parameters, both photometric and spectroscopic data are needed. Radial velocity analysis enables the determination of exact orbital parameters, while light curve analysis provides the orbital inclination and radii of the stars relative to the semi-major axis. As a result of both analyses, precise fundamental stellar parameters such as mass (M) can be obtained. M is the most important parameter which determines the life of a star. Therefore, an accurate determination of M is essential. In addition to M, metallicity also affects the life of a star. Hence, for a comprehensive investigation of the binary evolution, both parameters should be obtained. Double-lined eclipsing binary systems provide an opportunity to derive these parameters. While a precise M can be obtained from the analysis of radial velocity and light curves, the metallicity can be determined by implementing special approaches like the spectral disentangling method (Simon & Sturm 1994).

Binary systems are thought to form in the same interstellar area and hence the component stars in a binary system should have the same chemical abundance pattern. However, recent detailed studies about eclipsing binary stars indicated that components in a binary system could have different chemical structures (e.g., Paunzen et al. 2018; Jeong et al. 2017). This result is very important for understanding the binary's evolution. The increased number of such samples will be effective. Therefore, in this s-

tudy, we present a detailed analysis of a suspected metallic-line eclipsing binary star, DV Boo.

DV Boo (HD 126031, $V = 7^{\rm m}.54$) was classified as an eclipsing binary system by *Hipparcos* data (ESA 1997). The star was defined as a metallic-line star by Bidelman (1988). Grenier et al. (1999) gave a spectral classification of A3kA7hF5m which signifies a chemically peculiar star. However, these spectral classifications could be suspected because the double-lined feature of DV Boo was later discovered by Carquillat et al. (2004). Carquillat et al. (2004) analyzed medium resolution (R∼20 000, 42 000) spectroscopic data to obtain the orbital parameters of the binary system. Additionally, they presented the analysis of the *Hipparcos* light curve to derive the fundamental stellar parameters. However, because of the low quality of the photometric data and less number of measured radial velocities for the secondary component (low-mass), these parameters could not be determined sensitively. DV Boo is also present in a list of candidate pulsating eclipsing binary stars (Soydugan et al. 2006). However, the pulsating nature (if it exists) of the star has not been discovered.

In this study, we introduce a detailed analysis of DV Boo which is believed to manifest chemically peculiar characteristics. The star also has enough and good spectroscopic and photometric public data to investigate the star thoroughly. A detailed analysis of the star will allow us to obtain the atmospheric chemical structure of both binary components in DV Boo.

The paper is organized as follows. Information about the considered spectroscopic and photometric data is given in Section 2. Analysis of the radial velocity measurements is presented in Section 3. We introduce a comprehensive spectral analysis in Section 4. The light curve analysis is provided in Section 5. Discussion and conclusions are presented in Section 6.

2 OBSERVATIONAL DATA

In this study, we referenced the public photometric and spectroscopic data of DV Boo. The system has photometric data in two different archives. First is the All Sky Automated Survey (ASAS) archive[1] (Pojmanski 2002). ASAS is a low budget project which aims to detect and identify variable stars. The project provides data taken with V- and I-bands. However, DV Boo has only V-band data in the ASAS archive. The second archive is the Kamogata/Kiso/Kyoto Wide-field Survey (KWS) archive[2] (Maehara 2014). This survey provides B-, V- and Ic-band data. However, DV Boo only has usable V- and Ic-band data in the archive. These available photometric data were gathered and scattered points beyond the 3σ level were removed for the light curve analysis.

Table 1 Information on the Spectroscopic Data. The Rightmost Column Lists the Range of S/N.

Instrument	Resolving power	Observation dates	Number of Spectra	S/N Range
ELODIE	42000	2001 – 2002	12	45 – 90
FEROS	48000	2016	6	100 – 135
HARPS	85000	2009 – 2013	8	80 – 140

The spectroscopic data of DV Boo are available in ELODIE[3] and European Southern Observatory (ESO)[4] archives. In the ELODIE archive, there are twelve spectra of DV Boo. ELODIE is an échelle spectrograph which was mounted at the 1.93-m telescope at the Observatoire de Haute-Provence (France). The spectrograph provided spectra with a resolving power of ∼42 000 and with a wavelength range of $3850-6800$ Å (Moultaka et al. 2004). The ELODIE spectra are served after an automatic data reduction by the dedicated pipeline. All available reduced ELODIE spectra of DV Boo were compiled for analysis in this study.

The ESO archive provides the data taken from the ESO instruments at La Silla Paranal observatory. In this archive, there are six FEROS and eight HARPS spectra of DV Boo. FEROS and HARPS are échelle spectrographs and they are attached to the 2.2-m and the 3.6-m telescopes, respectively. FEROS has a resolving power of 48 000 and its spectral range is approximately between 3500 and 9200 Å (Kaufer et al. 1999). HARPS has a higher resolving power (85 000) and it supplies spectra in a wavelength range of about $3780 - 6900$ Å (Mayor et al. 2003). The spectra of FEROS and HARPS were reduced and calibrated by their dedicated pipelines. All available FEROS and HARPS spectra for DV Boo were incorporated into this study.

The collected reduced spectra were manually normalized applying the NOAO/IRAF[5] *continuum* task. Each spectrum was normalized separately and the continuum level was controlled with a synthetic spectrum that was generated using approximate atmospheric parameters. The information for the utilized spectroscopic data is given in Table 1. The average signal-to-noise ratio (S/N) of all spectroscopic data is ∼95.

3 RADIAL VELOCITY MEASUREMENTS

A binary system is defined with its orbital parameters such as inclination i, eccentricity e, semi-major axis a and argument of periastron w. To obtain accurate orbital parame-

[1] http://www.astrouw.edu.pl/asas
[2] http://kws.cetus-net.org/$\sim$maehara/VSdata.py
[3] http://atlas.obs-hp.fr/elodie/
[4] http://archive.eso.org
[5] http://iraf.noao.edu/

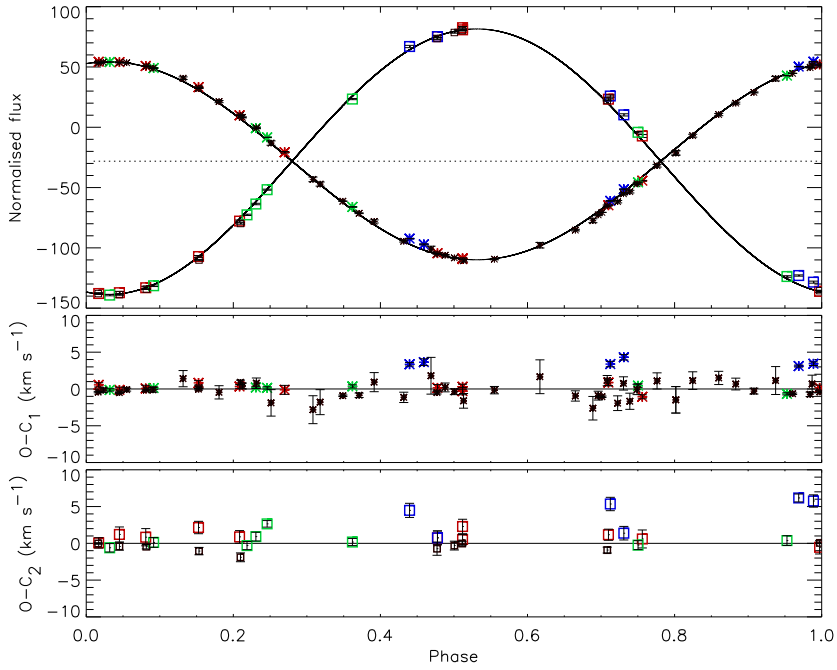

Fig. 1 Theoretical fits (*solid lines*) to the radial velocity measurements of the primary (*asterisks*) and the secondary (*squares*) components are plotted in the upper panel. The *red*, *blue*, *green* and *black symbols* illustrate the ELODIE, FEROS, HARPS and literature values (Carquillat et al. 2004), respectively. The *dashed line* in the upper panel signifies the Vγ level. The residuals from the fits are displayed in the lower panel. The subscripts "1" and "2" represent the primary and the secondary components, respectively.

ters of an eclipsing binary system, radial velocity measurements spread over the entire orbital phases are required.

The radial velocity (v_r) measurements of DV Boo were obtained by using the available public spectra. The IRAF FXCOR task was applied in the measurements. In this analysis, a radial velocity standard star, which has spectra acquired by the same instruments as for DV Boo, was taken into account. HD 693 was chosen as a template star. We calculated the v_r value of HD 693 as 15.18 km s^{-1} on average which is similar to the literature value (v_r = 14.81 km s^{-1}, Maldonado et al. 2010). As a result, the v_r values of DV Boo were acquired and they are listed in Table A.1.

After the v_r measurements, we derived the orbital parameters of DV Boo using the `rvfit` code[6]. This code calculates the theoretical v_r curves by implementing the adaptive simulated annealing method (Iglesias-Marzoa et al. 2015). For the analysis, we took the orbital period (P_{orb}) and periastron passage time (T_0) from Kreiner (2004). We also included the v_r measurements reported by Carquillat et al. (2004). The analysis was carried out using 74 v_r measurements in total. During the analysis, only the P_{orb} parameter was fixed and e, w, T_0, the velocity of the mass center Vγ and the amplitude of v_r curve of the star relative to the center of the binary mass K parameters were adjusted. The resulting parameters are listed in Table 2 and the theoretical v_r fit to the observed ones is displayed in Figure 1.

[6] *http://www.cefca.es/people/riglesias/rvfithtml*

Table 2 The Results of the Radial Velocity Analysis

Parameters	Value
P^a (d)	3.7826330
T_0 (HJD)	2450003.58014 ± 0.01523
e	0.004 ± 0.001
ω (deg)	347 ± 3
Vγ (km s^{-1})	–28.12 ± 0.03
K_1 (km s^{-1})	82.08 ± 0.04
K_2 (km s^{-1})	110.08 ± 0.07
$M_1 \sin^3 i$ ($M_\odot$)	1.593 ± 0.002
$M_2 \sin^3 i$ ($M_\odot$)	1.188 ± 0.002
$q = M_2/M_1$	0.7457 ± 0.0007
$a_1 \sin i$ (10^6 km)	4.2696 ± 0.0024
$a_2 \sin i$ (10^6 km)	5.7256 ± 0.0039

[a] Signifies fixed parameters.

4 SPECTRAL ANALYSIS

We aim to obtain the atmospheric parameters and chemical compositions of both binary components of DV Boo to examine their chemical structure and binary evolution. Therefore, in this section, we first disentangle the compos-

Table 3 Results of the Spectroscopic Analysis of the Individual Spectra of Binary Components

	H_γ line	Fe lines				
Star	$T_{\rm eff}$ (K)	$T_{\rm eff}$ (K)	log g (cgs)	ξ (km s^{-1})	$v \sin i$ (km s^{-1})	log ϵ (Fe)
DV Boo$_1$	7100 ± 230	7400 ± 100	4.1 ± 0.1	2.7 ± 0.2	26 ± 2	7.79 ± 0.25
DV Boo$_2$	6500 ± 360	6500 ± 100	4.3 ± 0.2	3.7 ± 0.3	17 ± 3	7.62 ± 0.32

The subscripts 1 and 2 represent the primary and secondary binary components, respectively.

ite spectra of the system and obtain the individual spectra of binary components. Then, we carry out a detailed spectroscopic analysis using these disentangled spectra.

4.1 Spectral Disentangling

The spectral disentangling method can be employed to acquire individual spectra of binary components in a double-lined (SB2) eclipsing binary system. To obtain the individual spectra of binary components, the composite spectra of the binary system taken in different orbital phases and the fractional light contribution of binary components are needed. To obtain initial fractional lights of the binary components, we performed a preliminary light curve analysis using the ASAS data. In the initial light curve analysis, effective temperature ($T_{\rm eff}$) value of the primary component was fixed. This $T_{\rm eff}$ value was estimated with the following steps. First, the *Gaia* distance (Gaia Collaboration et al. 2018) was utilized to estimate the interstellar absorption coefficient ($A_v = 0.062$, Schlafly & Finkbeiner 2011) and we calculated the $(B-V)_0$ value to be 0.31 mag. By considering the derived $(B-V)_0$ and the list given by Eker et al. (2018) (see table 7 in that article), we estimated the initial $T_{\rm eff}$ value of the primary binary component to be 7161 K. As a result of the preliminary light curve analysis, we determined the light contributions to be around 80% and 20% for the primary and secondary components, respectively. The final light curve analysis will be provided after accurate $T_{\rm eff}$ values are obtained.

The `FDBINARY` (Ilijic et al. 2004) code was used to obtain the individual spectra of the binary components. `FDBINARY` disentangles the composite spectra based on Fourier space by taking into account some orbital parameters such as P, T_0, $K_{1,2}$, e and ω. These orbital parameters can be fixed or adjusted during the analysis. However, the fractional light contributions of the binary components should be fixed in the analysis according to the orbital phases of the binary system in the considered spectra.

In the analysis, we used FEROS spectra because these data have significantly higher S/N on average relative to HARPS and ELODIE data. Additionally, available FEROS spectra are also distributed well over the orbital phases of DV Boo for the disentangling analysis.

In the analysis, the spectral range of around $4200 - 5600$ Å was taken into account. This spectral window was divided into several spectral subsets with $150 - 250$ Å steps. These spectral subsets were analyzed separately. In the analysis, the input parameters were taken from the results of the radial velocity analysis and they were fixed. Only the T_0 parameter was adjusted during the spectral disentangling process. After the individual spectra of binary components were obtained, these spectra were normalized considering each component star's light fraction (Pavlovski & Hensberge 2005).

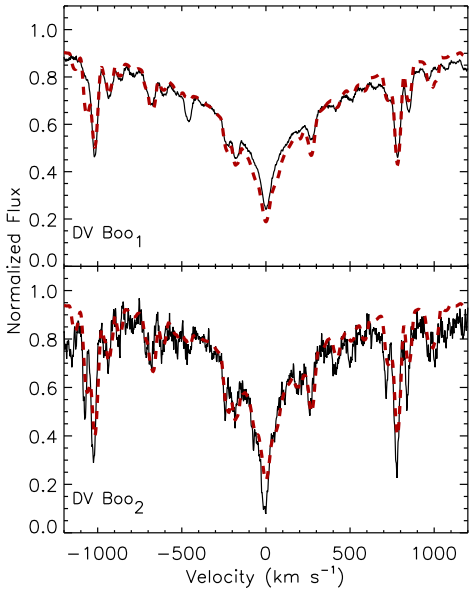

Fig. 2 Theoretical fits (*dashed lines*) to the observed H_γ lines. The subscripts "1" and "2" represent the primary and secondary binary components, respectively.

The S/N of the resulting individual spectra of the binary components can be calculated applying the equation given by Pavlovski & Southworth (2009). When we calculated the S/N, we found that the spectra of the primary and secondary binary components have S/N around 290 and 38 S/N, respectively. The S/N for the secondary component is low because of its less light contribution in total. Therefore, we are only able to determine the atmospheric parameters and metallicity value for the secondary star with this low S/N. A detailed abundance analysis will not be carried out for the secondary star.

Table 4 Abundances of Individual Elements of the Primary Star and Sun (Asplund et al. 2009)

Elements	Star abundance	Solar abundance
$_{6}$C	8.78 ± 0.44 (1)	8.43 ± 0.05
$_{11}$Na	6.68 ± 0.44 (1)	6.24 ± 0.04
$_{12}$Mg	7.90 ± 0.40 (4)	7.60 ± 0.04
$_{14}$Si	7.94 ± 0.39 (5)	7.51 ± 0.03
$_{20}$Ca	5.85 ± 0.41 (3)	6.34 ± 0.04
$_{21}$Sc	1.57 ± 0.41 (3)	3.15 ± 0.04
$_{22}$Ti	5.01 ± 0.37 (15)	4.95 ± 0.05
$_{23}$V	4.51 ± 0.42 (2)	3.93 ± 0.08
$_{24}$Cr	6.00 ± 0.37 (15)	5.64 ± 0.04
$_{25}$Mn	5.80 ± 0.39 (5)	5.43 ± 0.05
$_{26}$Fe	7.79 ± 0.25 (83)	7.50 ± 0.04
$_{28}$Ni	6.82 ± 0.37 (19)	6.22 ± 0.04
$_{30}$Zn	5.06 ± 0.44 (1)	4.56 ± 0.05
$_{38}$Sr	4.14 ± 0.45 (1)	2.87 ± 0.07
$_{39}$Y	4.14 ± 0.44 (1)	2.58 ± 0.07
$_{40}$Zr	4.62 ± 0.43 (2)	2.58 ± 0.04
$_{56}$Ba	3.59 ± 0.44 (1)	2.18 ± 0.07

Number of analyzed spectral parts is expressed in the Brackets.

4.2 Determination of the Atmospheric Parameters and Abundance Analysis

To determine the atmospheric parameters ($T_{\rm eff}$, surface gravity $\log g$, microturbulence ξ) and projected rotational velocity ($v \sin i$) of both binary components, we followed two different approaches. First, the H_γ line was taken into account to derive the $T_{\rm eff}$ parameter because hydrogen lines are very sensitive to $T_{\rm eff}$. It is also known that for cool stars ($T_{\rm eff} < 8000$ K) hydrogen lines are not sensitive to $\log g$ (Smalley et al. 2002; Smalley 2005). Hence, in the hydrogen line analysis, we took $\log g$ to be 4.0 cgs and additionally we assumed solar metallicity, as metallicity does not change the profile of hydrogen lines. The H_γ $T_{\rm eff}$ values were derived considering the minimum difference between the synthetic and observed spectra. During this and future spectral analyses, the hydrostatic, plane-parallel and line-blanketed local thermodynamic equilibrium (LTE) ATLAS9 model atmospheres (Kurucz 1993) were used. The synthetic spectra were generated by SYNTHE code (Kurucz & Avrett 1981). The errors in the H_γ $T_{\rm eff}$ values were estimated considering the 1σ difference in χ^2 and also taking into account possible uncertainty that comes from normalization ($\sim$100 K, Kahraman Aliçavuş, in preparation). The resulting H_γ $T_{\rm eff}$ values are expressed in Table 3 and the theoretical fits to the H_γ lines are depicted in Figure 2.

All atmospheric parameters were determined following another approach. In this approach, the excitation and ionization potential balances of iron (Fe) lines were taken into account. In this method, some small spectral parts ($1 - 5$ Å) were analyzed separately based on the spectral synthesis method. The final $T_{\rm eff}$, $\log g$ and ξ parameters were searched in the range of $6000 - 7600$ K, $3.8 - 4.5$ cgs and $1 - 4$ km s^{-1} with 100 K, 0.1 cgs and 0.1 km s^{-1} steps, respectively. By employing the given input parameters, we adjusted Fe abundances and $v \sin i$ parameters considering the minimum difference between the theoretical and observed spectra. The final $T_{\rm eff}$ and $\log g$ parameters were derived considering the relationships between Fe abundance and excitation/ionization potentials. For the correct atmospheric parameters, these relationships should be flat because the abundance of the individual elements obtained from different lines should be the same for different excitation potentials. Additionally, the ξ value was obtained utilizing the same abundance – excitation potential relationship as explained by Sousa (2014). For a detailed explanation of the employed method, check the studies of Kahraman Aliçavuş et al. (2016) and Niemczura et al. (2015).

In analysis of the primary component, 59 neutral and 24 ionized suitable Fe lines were used, while these numbers are 36 (FeI) and 15 (FeII) for the secondary component. The uncertainties in the determined final atmospheric parameters were obtained by the 1σ change in the associated relationships. We calculated how much the atmospheric parameters alter with the 1σ difference in the considered relationships. The final atmospheric parameters and their uncertainties are given in Table 3.

After the final atmospheric parameters were determined, abundance analysis was carried out taking these parameters as input. However, we only performed this analysis for the primary component, because the secondary component has a low S/N for an abundance analysis. We only obtained $\log \epsilon$ (Fe) for the secondary component using the Fe lines because Fe lines are abundant and dominate in the secondary star's $T_{\rm eff}$ range. For abundance analysis of the primary component, first a line identification was done for each spectral part using the Kurucz line list[7] and then all parts were analyzed separately. The chemical abundances determined from the different spectral parts were taken into account to obtain the average individual chemical abundances. The list of final chemical abundances for the primary component is provided in Table 4. The uncertainties in the chemical abundances were estimated considering the effects of quality of the spectrum (S/N, resolution), errors in the atmospheric parameters and assumptions in the model atmosphere calculations. The effect of the LTE model assumption on chemical abundance calculations was searched by Mashonkina (2011) and it turned out that these assumptions introduce around a 0.1 dex error. The effects of S/N and resolution were examined by Kahraman Aliçavuş et al. (2016) in detail. We took into account the errors caused by these sources from this study. Additionally, we calculated the errors caused by uncertainties in the determined atmospheric parameters. The

[7] kurucz.harvard.edu/linelists.html

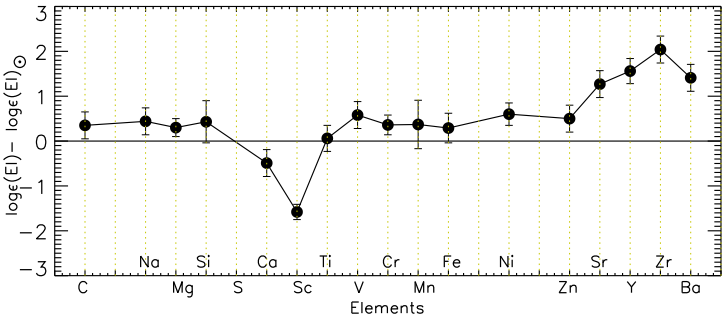

Fig. 3 Chemical abundance distribution of the primary binary component relative to solar abundance (Asplund et al. 2009).

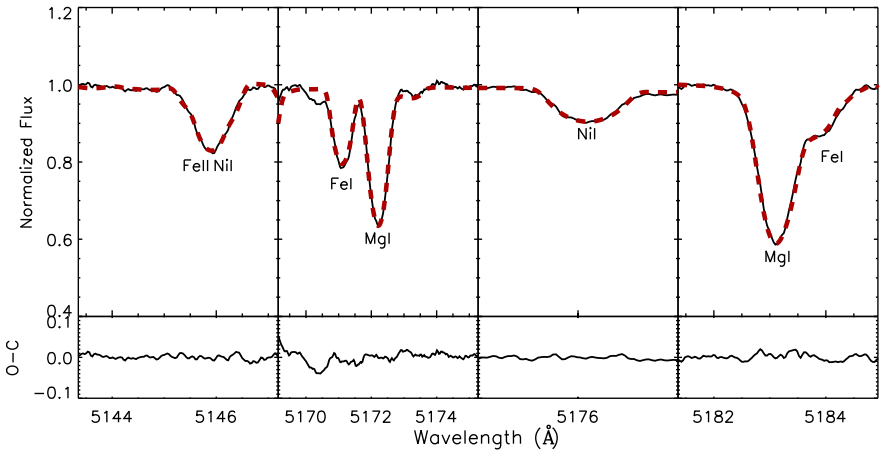

Fig. 4 Theoretical fits (*dashed lines*) to the disentangled spectrum (*solid lines*) of the primary binary component (*upper panels*) and the residuals ($O - C$) (*lower panels*).

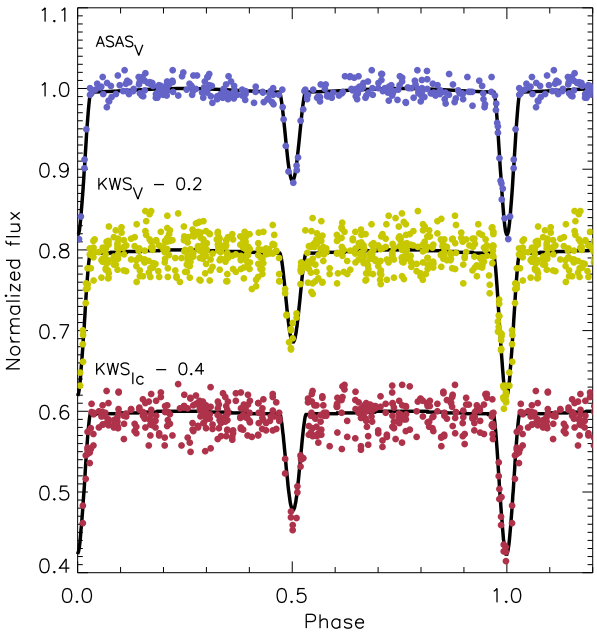

Fig. 5 Theoretical light curve fits (*solid lines*) to the observed public photometric data (*points*) of DV Boo.

Table 5 Results of the Light Curve Analysis and the Astrophysical Parameters

Parameter	Value
i (deg)	82.995 ± 0.251
$T_1{}^a$ (K)	7400 ± 100
T_2 (K)	6398 ± 174
V_γ (km s^{-1})	-28.11 ± 0.03
a ($R_\odot$)	14.469 ± 0.010
e^a	0.004 ± 0.001
Ω_1	8.100 ± 0.223
Ω_2	9.499 ± 0.277
Phase shift	0.0004 ± 0.0001
q^a	0.746 ± 0.001
$r_1{}^*$ (mean)	0.1359 ± 0.0036
$r_2{}^*$ (mean)	0.0889 ± 0.0026
L_1 / (L_1+L_2) (ASAS)	0.797 ± 0.016
L_1 / (L_1+L_2) (KWS V)	0.797 ± 0.016
L_1 / (L_1+L_2) (KWS I)	0.778 ± 0.016
L_2 /(L_1+L_2) (ASAS)	0.203 ± 0.016
L_2 /(L_1+L_2) (KWS V)	0.203 ± 0.016
L_2 /(L_1+L_2) (KWS I)	0.222 ± 0.016
l_3	0.0
Derived Quantities	
M_1 ($M_\odot$)	1.629 ± 0.004
M_2 ($M_\odot$)	1.215 ± 0.003
R_1 ($R_\odot$)	1.966 ± 0.052
R_2 ($R_\odot$)	1.286 ± 0.038
log ($L_1/L_\odot$)	1.020 ± 0.033
log ($L_2/L_\odot$)	0.398 ± 0.054
log g_1 (cgs)	4.063 ± 0.023
log g_2 (cgs)	4.304 ± 0.025
$M_{\rm bolometric1}$ (mag)	2.201 ± 0.082
$M_{\rm bolometric2}$ (mag)	3.755 ± 0.134
M_{V1} (mag)	2.166 ± 0.086
M_{V2} (mag)	3.759 ± 0.143
Distance (pc)	130 ± 5

The subscripts 1, 2 and 3 represent the primary, secondary and third binary components, respectively.
^{a} Signifies fixed parameters; * fractional radii.

quadrature sum of the errors introduced by the uncertainties in the atmospheric parameters was found to be around 0.15 dex. The final calculated uncertainties are listed in Table 4.

5 LIGHT CURVE ANALYSIS

In the light curve analysis, the normalized V-band ASAS and V- and Ic-bands KWS photometric data were included. The analysis was carried out utilizing the Wilson-Devinney (Wilson & Devinney 1971) code which was integrated with a Monte Carlo (MC) simulation to precisely estimate uncertainties in the adjusted parameters (Zola et al. 2004, 2010).

During the analysis, some parameters were adjusted while some were fixed. The $T_{\rm eff}$ value of the primary star was set as 7400 K from the present spectroscopic analysis. In addition to the primary star's $T_{\rm eff}$ value, the logarithmic limb darkening coefficients taken from van Hamme (1993) were fixed and also the bolometric albedos (A, Ruciński 1969) and the bolometric gravity-darkening coefficients (g, von Zeipel 1924) were fixed according to the assumption of convective and radiative atmospheres. We assumed these A and g values to be 1 for the primary component and respectively 0.5 and 0.32 for the secondary component. The parameters q, e, and ω determined in the radial velocity analysis were also fixed. Additionally, the detached binary configuration was considered in the analysis. We adjusted the phase shift, i, secondary component's $T_{\rm eff}$, dimensionless potentials (Ω) and the light fractions of binary components. As a result, we obtained the parameters of the binary system. No third light contribution was found. The obtained values and their uncertainties calculated by the MC method are provided in Table 5. The theoretical fits to the photometric data are presented in Figure 5. The fundamental stellar parameters were also calculated employing the `JKTABSDIM` code (Southworth et al. 2004). These parameters are also listed in Table 5.

6 DISCUSSION AND CONCLUSIONS

In this study, we present a detailed photometric and spectroscopic study of an eclipsing binary system DV Boo. The fundamental atmospheric parameters of binary components were obtained by using the disentangled spectra of each component. DV Boo was classified as a metallic-line (Am) star. According to our chemical abundance analysis, we found that the primary component exhibits typical Am star properties (see, Fig. 4). The primary star has mostly overabundant iron-peak elements and manifests deficiency in Ca and Sc elements. This is a typical chemical abundance behavior of Am stars. It is known that many (∼70%) Am stars are members of binary systems (Carquillat & Prieur 2007). However, eclipsing binary Am stars are rare (Smalley et al. 2014). Therefore, the current detailed analysis of DV Boo is important to thoroughly understand Am stars' behavior. Additionally, we found that the secondary binary component also has a similar Fe abundance with the primary star.

When the obtained atmospheric parameters were examined, we noticed that the secondary binary component has a higher ξ value compared to the ξ range for a star with similar $T_{\rm eff}$ value (Gebran et al. 2014; Landstreet et al. 2009). However, we keep in mind that our star is a member of a binary system and there are interactions between the two binary components. Therefore, the reason for the resulting ξ value could be the effect of binarity. This should be investigated in further studies.

A light curve analysis was performed utilizing the ASAS V-band and KWS V- and Ic-band data. As a result, we derived the orbital and fundamental stellar parameters. The M values of the binary components were obtained with an accuracy of less than 1%, while the accuracy in R values is less than 3%. These precise M and R values allow us to examine the evo-

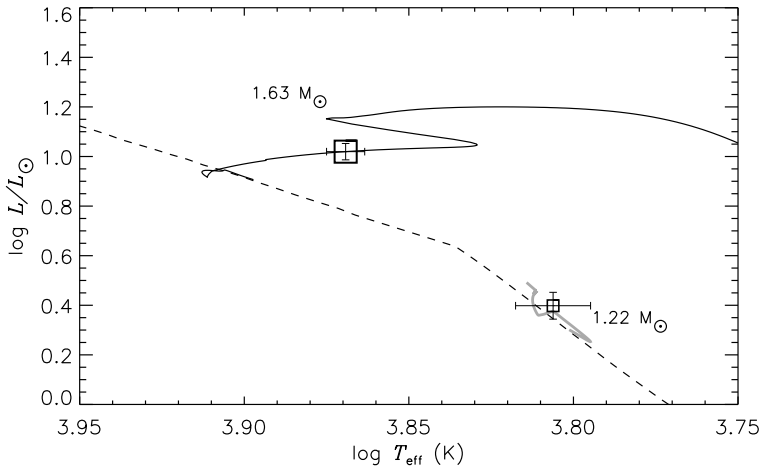

Fig. 6 The positions of the primary and secondary (smaller symbol) binary components of DV Boo in the H-R diagram. *Solid black* and *grey lines* represent the evolutionary tracks for primary and secondary components, respectively. The *dashed line* illustrates the ZAMS.

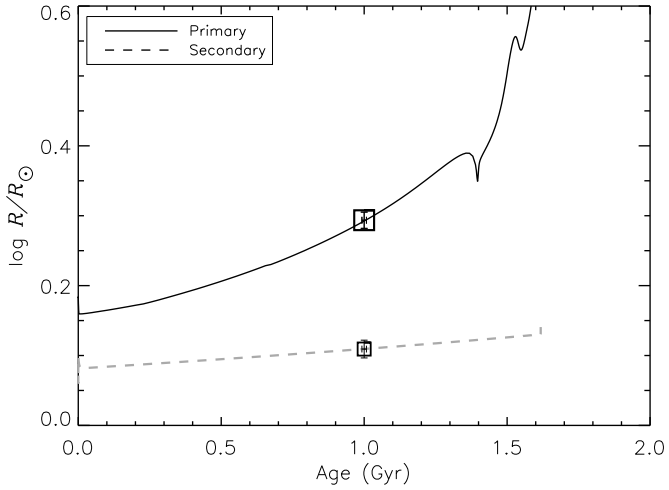

Fig. 7 The position of the primary and secondary (smaller symbol) binary components of DV Boo in the Age – log R diagram.

Table 6 Evolutionary Model Parameters Obtained from MESA

Parameter	Value
$P_{\rm initial}$ (d)	3.895 ± 0.020
$e_{\rm initial}$	0.023 ± 0.003
Z	0.015 ± 0.002
Age (Gyr)	1.00 ± 0.08

lutionary status of DV Boo. Therefore, the evolutionary status of DV Boo was examined by employing the 8845 version of the `Modules for Experiments in Stellar Astrophysics` (MESA) evolutionary program (Paxton et al. 2011, 2013). The binary module of MESA (Paxton et al. 2015) was used to estimate the initial evolutionary parameters of the binary system and to model its orbital evolution. Many evolutionary models were generated with different input parameters. During the analysis, the metallicity (Z) value was searched between 0.01 and 0.02 with steps of 0.001. As a result, $Z = 0.015 \pm 0.002$ was found. According to current spectroscopic analysis, the binary components of DV Boo have Z value around solar ($Z = 0.0143$, Asplund et al. 2009) within error bars. This Z value is consistent with the Z value obtained from evolutionary models. Additionally, we estimated the initial orbital period and e value by comparing the models calculated with different input orbital parameters and e.

The resulting evolutionary models for primary and secondary binary components were estimated taking into account the best fit to the calculated Age – log R diagram. As a result, we defined the age of components to be 1.00 ± 0.08 Gyr and examined the orbital evolution of the binary system. The first Roche lobe overflow (RLOF) time

for the primary component of DV Boo is predicted to start at the age of 1.61 Gyr (0.61 Gyr after the current age). The system is expected to become a semi-detached binary after this age with the beginning of rapid mass transfer. In this stage, the secondary component will gain mass and it will evolve parallel to the zero age main sequence (ZAMS) by its increasing radius and luminosity due to the mass transfer. The best fit evolutionary models for the binary components of DV Boo and the position of the components in the Hertzsprung-Russell (H-R) diagram are plotted in Figure 6. Furthermore, the location of the components in the Age – log R diagram is illustrated in Figure 7. In these figures, the binary components' evolutionary models are shown from zero-age to the early stage of the beginning of mass transfer. The estimated initial evolutionary parameters are given in Table 6.

In the light curve analysis, a synchronous rotation was assumed. If the binary components are synchronized, their $v \sin i$ values should be 26.3 ± 0.7 and 17.2 ± 0.5 km s^{-1} for the primary and secondary components, respectively. These values are very similar to the spectroscopic ones. This shows us the binary components are already synchronized. In addition to this, applying the resulting parameters of the light curve analysis, we estimated the distance of DV Boo to be 130 ± 5 pc which is consistent with the *Gaia* distance ($\sim$125 pc, Gaia Collaboration et al. 2018).

DV Boo is included in the list of candidate δ Scuti-type variables in eclipsing binaries (Soydugan et al. 2006). Therefore, we carried out a frequency analysis of the photometric data after removing the binary light variation. The `Period04` code (Lenz & Breger 2005) was employed in the analysis. We found some frequency peaks at δ Scuti stars' pulsation frequency regime. However, the data are not good enough to classify the primary star to be a δ Scuti variable. Better quality data are needed.

The present detailed study of DV Boo offers good input data to examine the evolution of binary systems and to understand the characteristic of Am stars in binaries. This kind of spectroscopic analysis of eclipsing binary systems is required for a comprehensive investigation of binary evolution.

Acknowledgements The authors would like to thank the reviewer for his/her useful comments and suggestions. FKA thanks the Polish National Center for Science (NCN) for supporting the study through grant 2015/18/A/ST9/00578. We thank Prof. G. Handler for his helpful comments. The calculations were carried out at the Wrocław Centre for Networking and Supercomputing (`http://www.wcss.pl`), grant No. 214. This research has made use of the SIMBAD database, operated at CDS, Strasbourg, France. This study is based on data obtained from the ESO Science Archive Facility under request number 524778 by Filiz Kahraman Alicavus and based on spectral data retrieved from the ELODIE archive at Observatoire de Haute-Provence (OHP, `http://atlas.obs-hp.fr/elodie/`). This work has made use of data from the European Space Agency (ESA) mission *Gaia* (`https://www.cosmos.esa.int/gaia`), processed by the *Gaia* Data Processing and Analysis Consortium (DPAC, `https://www.cosmos.esa.int/web/gaia/dpac/consortium`). Funding for the DPAC has been provided by national institutions, in particular the institutions participating in the *Gaia* Multilateral Agreement.

Appendix A:

Table A.1 The v_r Measurements

HJD +2450000	$v_{r,1}$ (km s^{-1})	$v_{r,2}$ (km s^{-1})	Instrument
1931.6262	–64.71 ± 0.42	23.28 ± 0.76	ELODIE
2039.4253	9.91 ± 0.25	–77.80 ± 0.86	ELODIE
2040.5722	–108.66 ± 0.34	80.82 ± 0.66	ELODIE
2040.5722	–109.26 ± 0.48	82.58 ± 0.98	ELODIE
2041.4968	–44.32 ± 0.27	–7.24 ± 1.20	ELODIE
2042.4086	52.12 ± 0.37	–136.04 ± 0.91	ELODIE
2042.5900	53.97 ± 0.37	–137.16 ± 1.02	ELODIE
2043.4398	–20.74 ± 0.61		ELODIE
2297.6622	–104.46 ± 0.44	75.21 ± 0.94	ELODIE
2299.7025	54.31 ± 0.29	–137.86 ± 0.71	ELODIE
2303.7271	50.83 ± 0.43	–133.06 ± 1.17	ELODIE
2489.3476	33.27 ± 0.31	–107.19 ± 0.84	ELODIE
6473.5455	–92.34 ± 0.24	66.98 ± 0.96	FEROS
6473.6190	–97.12 ± 0.46	75.00 ± 0.46	FEROS
6474.5781	–61.04 ± 0.37	25.91 ± 0.91	FEROS
6474.6475	–51.43 ± 0.37	10.29 ± 0.92	FEROS
6475.5470	50.30 ± 0.14	–122.94 ± 0.53	FEROS
6475.6228	54.41 ± 0.24	–128.43 ± 0.84	FEROS
4887.8319	–0.75 ± 0.16	–63.65 ± 0.60	HARPS
4887.8897	–8.37 ± 0.16	–51.76 ± 0.45	HARPS
4889.7976	–45.72 ± 0.26	–4.16 ± 0.61	HARPS
4890.8627	54.12 ± 0.16	–139.19 ± 0.57	HARPS
5431.4800	42.81 ± 0.16	–123.75 ± 0.66	HARPS
5432.4855	–6.19 ± 0.18	–72.62 ± 0.55	HARPS
6449.5334	49.12 ± 0.17	–131.41 ± 0.66	HARPS
6450.5559	–66.05 ± 0.21	–23.39 ± 0.49	HARPS

The subscripts "1" and "2" represent the primary and the secondary components, respectively.

References

Asplund, M., Grevesse, N., Sauval, A. J., et al. 2009, ARA&A, 47, 481

Alfonso-Garzón, J., Montesinos, B., Moya, A., et al. 2014, MNRAS, 443, 3022

Bidelman, W. P. 1988, PASP, 100, 1084

Carquillat, J.-M., Prieur, J.-L., Ginestet, N., et al. 2004, MNRAS, 352, 708

Carquillat, J.-M., & Prieur, J.-L. 2007, MNRAS, 380, 1064

Eker, Z., Bakış, V., Bilir, S., et al. 2018, MNRAS, 479, 5491
ESA 1997, ESA Special Publication
Gaia Collaboration, Brown, A. G. A., Vallenari, A., et al. 2018, A&A, 616, A1
Gebran M., Monier R., Royer F., Lobel A., Blomme R., 2014, psce.conf, 193
Grenier, S., Baylac, M.-O., Rolland, L., et al. 1999, A&AS, 137, 451
Iglesias-Marzoa, R., López-Morales, M., & Jesús Arévalo Morales, M. 2015, PASP, 127,567
Ilijic, S., Hensberge, H., Pavlovski, K., et al. 2004, Spectroscopically and Spatially Resolving the Components of the Close Binary Stars, 111
Jeong, Y., Yushchenko, A. V., Doikov, D. N., et al. 2017, Journal of Astronomy and Space Sciences, 34, 75
Kahraman Aliçavuş, F., Niemczura, E., De Cat, P., et al. 2016, MNRAS, 458, 2307
Kaufer, A., Stahl, O., Tubbesing, S., et al. 1999, The Messenger, 95, 8
Kreiner, J. M. 2004, Acta Astronomica, 54, 207
Kurucz, R. L., & Avrett, E. H. 1981, SAO Special Report, 391
Kurucz, R. 1993, ATLAS9 Stellar Atmosphere Programs and 2 km/s Grid (Cambridge: Kurucz CD-ROM), 13
Landstreet, J. D., Kupka F., Ford, H. A., Officer, T., et al. 2009, A&A, 503, 973
Lenz, P., & Breger, M. 2005, Communications in Asteroseismology, 146, 53
Maehara, H., 2014, Journal of Space Science Informatics Japan, 3, 119, *https://ci.nii.ac.jp/naid/110009799479*
Maldonado, J., Martínez-Arnáiz, R. M., Eiroa, C., et al. 2010, A&A, 521, A12
Mashonkina, L. 2011, Magnetic Stars, 314
Mayor, M., Pepe, F., Queloz, D., et al. 2003, The Messenger, 114, 20
Moultaka, J., Ilovaisky, S. A., Prugniel, P., et al. 2004, PASP, 116, 693
Niemczura, E., Murphy, S. J., Smalley, B., et al. 2015, MNRAS, 450, 2764
Paunzen, E., Fedurco, M., Hełminiak, K. G., et al. 2018, A&A, 615, A36
Paxton, B., Bildsten, L., Dotter, A., et al. 2011, ApJS, 192, 3
Paxton, B., Cantiello, M., Arras, P., et al. 2013, ApJS, 208, 4
Paxton, B., Marchant, P., Schwab, J., et al. 2015, ApJS, 220, 15
Pavlovski, K., & Hensberge, H. 2005, A&A, 439, 309
Pavlovski, K., & Southworth, J. 2009, MNRAS, 394, 1519
Pojmanski, G. 2002, Acta Astronomica, 52, 397
Ruciński, S. M. 1969, Acta Astronomica, 19, 245
Sana, H., & Evans, C. J. 2011, Active OB Stars: Structure, Evolution, Mass Loss, and Critical Limits, 474
Schlafly, E. F., & Finkbeiner, D. P. 2011, ApJ, 737, 103
Sousa, S. G. 2014, in Determination of Atmospheric Parameters of B-, A-, F- and G- Type Stars, eds. E. Niemczura et al. (Cham: Springer Internatoinal Publishing), 297
Simon, K. P., & Sturm, E. 1994, A&A, 281, 286
Smalley, B., Gardiner, R. B., Kupka, F., et al. 2002, A&A, 395, 601
Smalley, B. 2005, Memorie della Societa Astronomica Italiana Supplementi, 8, 130
Smalley, B., Southworth, J., Pintado, O. I., et al. 2014, A&A, 564, A69
Southworth, J., Maxted, P. F. L., & Smalley, B. 2004, MNRAS, 351, 1277
Southworth, J. 2013, A&A, 557, A119
Soydugan, E., Soydugan, F., Demircan, O., et al. 2006, MNRAS, 370, 2013
Torres, G., Andersen, J., & Giménez, A. 2010, A&A Rev., 18, 67
van Hamme, W. 1993, AJ, 106, 2096
von Zeipel, H. 1924, MNRAS, 84, 665
Wilson, R. E., & Devinney, E. J. 1971, ApJ, 166, 605
Zola, S., Rucinski, S. M., Baran, A., et al. 2004, Acta Astronomica, 54, 299
Zola, S., Gazeas, K., Kreiner, J. M., et al. 2010, MNRAS, 408, 464